

GEOLOGY OF THE SOUTHERN OKANAGAN VALLEY SHEAR ZONE



Cover photo. View north along Okanagan Lake from Munson Mountain near Penticton (Fig. 1), showing the inferred trace of the Okanagan Valley fault (OVF). On the right (east) is the footwall and the west-dipping margin of the Okanagan Highlands capped by a carapace of Eocene Okanagan gneiss (Egn) overlying the (?) Eocene granodiorite of Okanagan Mountain (Eg). The dip slope is approximately the same orientation and attitude as the Okanagan Valley shear zone (OVSZ). On the left (west) is the hanging wall composed of Mesozoic metasedimentary rocks (not shown) overlain by tilted and folded Eocene sedimentary and volcanoclastic rocks of the Mamara and White Lake Formations (Em and Ewl). These sedimentary and volcanoclastic rocks were deposited into syn-tectonic, hanging wall half-graben (e.g., the White Lake Basin). The curved trace of the OVF and the geomorphic expression of the Okanagan Valley result from the development of km-scale, syn-extensional corrugations. Figure prepared by Dan Gibson (2009 GSA field guide).

This field guide has been adapted from one produced for a GSA Cordilleran Section fieldtrip (Kelowna - May 2009) led by Sarah Brown, Dan Gibson, and Derek Thorkelson, and SRB's PhD thesis completed at Simon Fraser University (Brown, 2010).

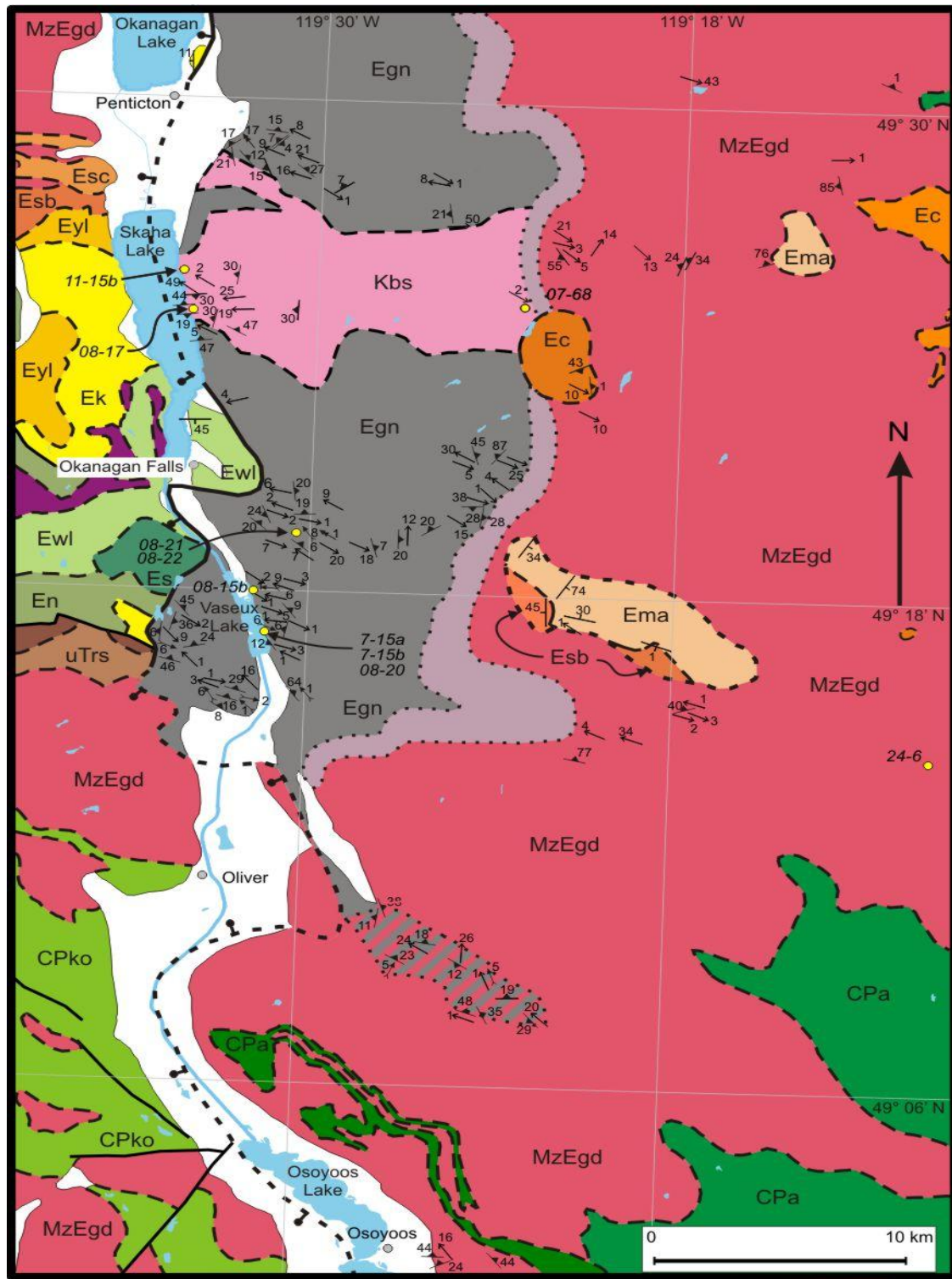


Figure 1a. Simplified geological map of the southern Okanagan Valley between Penticton (49°30'N) and the US-Canada border (49°N). The mapped or inferred trace of the OVF is shown as the heavy black line. The geological key is presented in Figure 1b (next page). Brown (2010).



Figure 1b. Schematic generalized vertical section color-coded as a lithological key for Figure 1a. Note that rocks in the upper plate (hanging wall) and lower plate (footwall) of the OVSZ are shown in different columns. Lithostratigraphic codes are adapted from Tempelman-Kluit (1989). Brown (2010).

Objectives

The purpose of this trip is to examine evidence for ductile extension and associated mylonitization within the Okanagan Valley shear zone, and to encourage discussion of shear zones and low-angle detachment faults, and the role they play in the formation of metamorphic core complexes, orogenic collapse and tectonic exhumation. We will discuss high-grade metamorphism, migmatization, mylonitization, pseudotachylite formation, and non-planar detachment fault surfaces.

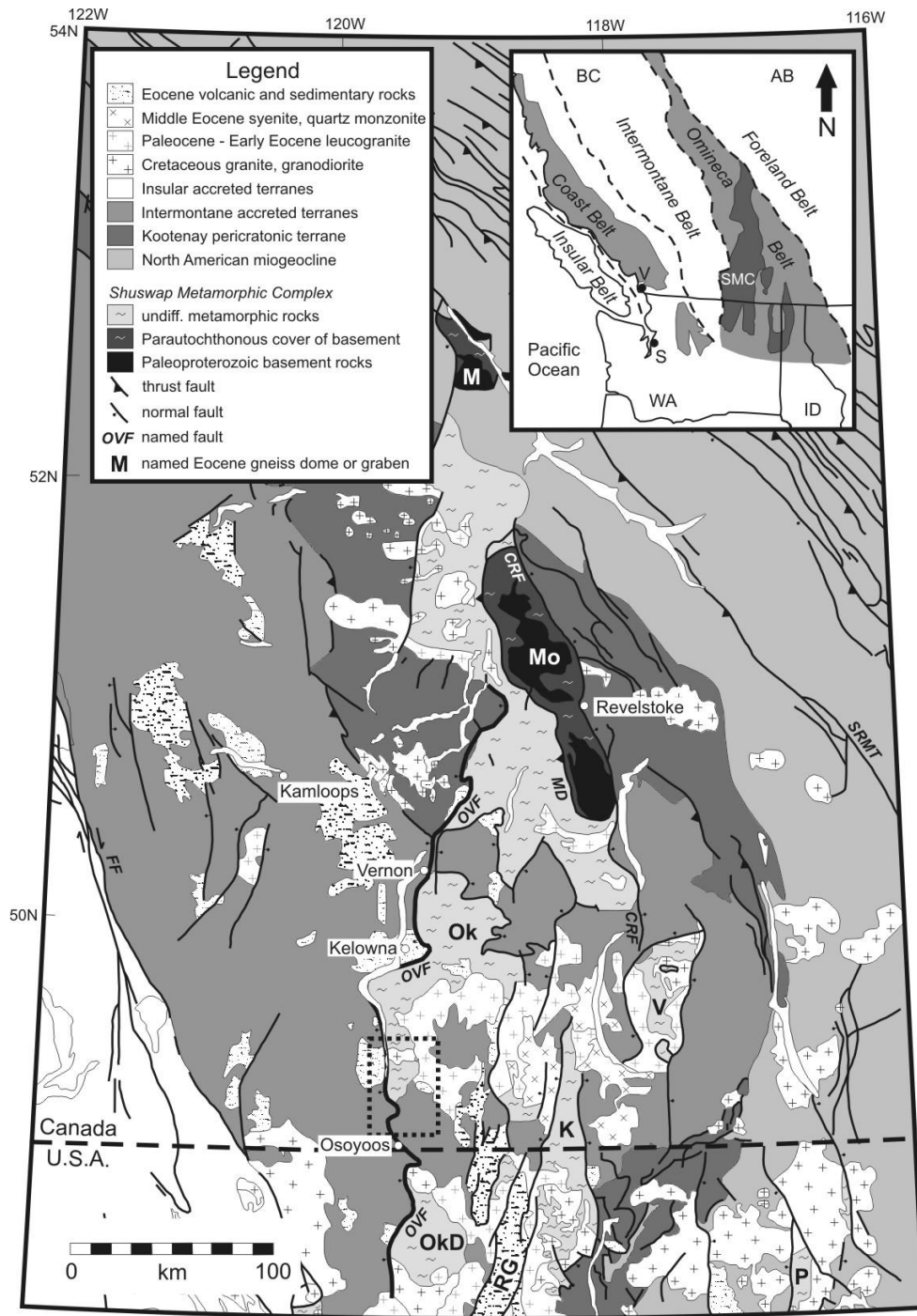


Figure 2. Simplified geological map showing the distribution of high-grade metamorphic and granitic rocks of the Shuswap metamorphic complex, and adjacent Paleozoic-Mesozoic tectono-stratigraphic belts and Eocene rocks. Abbreviations: K - Kettle River-Grand Forks dome, M - Malton gneiss, Mo - Monashee culmination, Ok - Okanagan complex, OkD - Okanagan Dome, P - Priest River complex, V - Valhalla dome, RG - Republic Graben; CRF - Columbia River fault, FF - Fraser fault, MD - Monashee décollement, OVF - Okanagan Valley fault, SRMT - Southern Rocky Mountain Trench. Inset: Position of

the Shuswap metamorphic complex (SMC) within the Omineca belt of the southern Canadian Cordillera; S - Seattle, V - Vancouver. Adapted from Johnson (2006) and Kruckenberg et al. (2008).

Introduction

This trip focuses on the southern portion of the Okanagan Valley fault (OVF) and adjacent gneisses in south-central British Columbia (Fig. 1a), within the Penticton map sheet (NTS map sheet 82E). The Okanagan Valley is broadly a north-south trending tectonic lineament that is over 300 km in length located in south-central BC and northern Washington (Fig. 2). It separates the Okanagan Highlands plateau to the east, from areas of generally lower elevation, but greater relief, to the west (see cover photo). The Valley is typically asymmetrical in cross-section, with a major west-dipping slope forming the western boundary of the Okanagan Highlands.

Regional Geological Context

The southern OVF system forms the southern boundary between the high-grade rocks of the Shuswap metamorphic complex within the southern Omineca Belt (to the east) and the allochthonous arc-related terranes of the Intermontane belt (to the west; Fig. 1). The gneisses of the Okanagan Highlands form part of the Shuswap metamorphic complex (SMC; Fig. 2). The SMC is situated in an extended region that has sillimanite-bearing upper amphibolite-facies rocks and Cretaceous to Eocene granitic intrusions. The SMC consists of Paleoproterozoic to Mesozoic, polydeformed, metasedimentary and metavolcanic rocks that were largely deposited on or near the western North American cratonic margin. To the west, rocks in the hanging wall of the OVF consist of zeolite to lower amphibolite-facies sedimentary and volcanic rocks of the Intermontane belt (Okulitch, 1979; Parkinson, 1985). Predominately, these are Late Proterozoic to Lower Jurassic rocks of oceanic and oceanic-arc affinity that have been intruded multiple times by pre-Triassic through Middle Eocene intrusive rocks.

The formation of the SMC gneisses corresponds to a period of tectonic thickening of the crust during the Mesozoic and Paleogene terrane accretion and orogenesis (Monger et al., 1982). There was a shift from compression to extension in the Omineca Belt in response to a change in Eocene plate boundary kinematics from transpressional to transtensional regime that facilitated post-orogenic collapse and exhumation of crystalline basement from depths of ≤ 30 km. During this time there was also widespread calc-alkaline and alkaline magmatism and volcanism, and the development of isolated syn-tectonic sedimentary basins. The SMC has a series of northerly striking extensional faults systems and transfer zones of early Paleogene age, including the OVF, (Parkinson, 1985; Templeman-Kluit and Parkinson, 1986; Parrish et al., 1988; Bardoux, 1993; Johnson and Brown, 1996; Glombick et al., 2006; Johnson 2006; see Table 1) for which varying amounts (0-90 km) of displacement have been inferred. Previous models, which include seismic profiles, have inferred that the OVF substantially penetrates the crust and served as a crustal-scale detachment that exhumed mid-crustal rocks (Templeman-Kluit and Parkinson, 1986; Parrish et al., 1988; Bardoux, 1993; Cook et al., 1992; Cook, 1995; Johnson and Brown, 1996).

Within the Penticton map sheet (NTS 82E), Tempelman-Kluit and Parkinson (1986) and Tempelman-Kluit (1989) documented a low angle, west dipping, brittle-ductile extensional fault which separated Upper Paleozoic and Triassic sub-greenschist to greenschist-facies metasedimentary and metavolcanic

rocks and Middle Eocene volcanic rocks in its hanging wall, from upper amphibolite-facies ortho- and paragneissic rocks in its footwall. The contact is not traceable along most of the Okanagan Valley as it lies underwater. However, in places where the contact is exposed it consists of a diffuse zone, 1-2 km thick, of highly sheared and deformed rocks, including mylonitized and brecciated gneisses that have been hydrothermally altered.

<div style="display: flex; align-items: center;"> <div style="writing-mode: vertical-rl; transform: rotate(180deg);"> Okanagan – Eagle River - North Thompson - Adams Lake fault system </div> <div style="margin: 0 10px;"> <div style="text-align: center;">north</div> <div style="text-align: center;">↑</div> <div style="text-align: center;">↓</div> <div style="text-align: center;">south</div> </div> </div>	Study area	Extension (km)	Authors
	Shuswap Lake	~30	Johnson, 1994
	Sicamous	32	Johnson & Brown, 1996
	Vernon	0 - <<12	Glombick, 2005; Glombick et al. 2006
	Kelowna	45 - 70	Bardoux, 1993
	southern OVF	10 - 60	Parkinson, 1985
	southern OVF	60 - 90	Tempelman-Kluit & Parkinson, 1986
	southern OVF	29 - 86	<i>this study</i>

Table 1. Estimates of down-to-the-west extension along the Okanagan Valley fault system, from north to south. Brown (2010).

Outstanding Issues / Controversies

The hypothesis that the OVF is a crustal-scale detachment has been challenged by recent studies in the Vernon area which show continuity in the superstructure across the proposed trace of the OVF (Thompson and Unterschutz 2004; Glombick et al. 2004; Glombick et al., 2006). These studies call into question the significance of low angle shear zones in the exhumation of the SMC and require a model (e.g. channel flow) that does not ascribe significant displacement to the OVF system, which seemingly contradicts determinations made at other locations along the OVF (Table 1). For example, Tempelman-Kluit and Parkinson (1986) correlated Eocene volcanic outliers in the upper plate with bodies of similar age (Coryell syenite) in the lower plate to come up with an estimate of 60-90 km of extension (upper plate to the west). Bardoux (1993) used palinspastically restored cross sections to determine 45-70 km of displacement in the Kelowna area; similarly, further north at the latitude of Sicamous, Johnson and Brown (1996) estimated ~32 km of displacement (see Table 1).

Clearly, a discrepancy exists amongst the models proposed for the exhumation of the SMC, mainly between the ‘classic’ core complex model (e.g., Coney, 1980; Armstrong, 1982; Coney and Harms, 1984; Tempelman-Kluit and Parkinson, 1986) and a mid-crustal ‘channel-flow’ model (e.g., Glombick et al.,

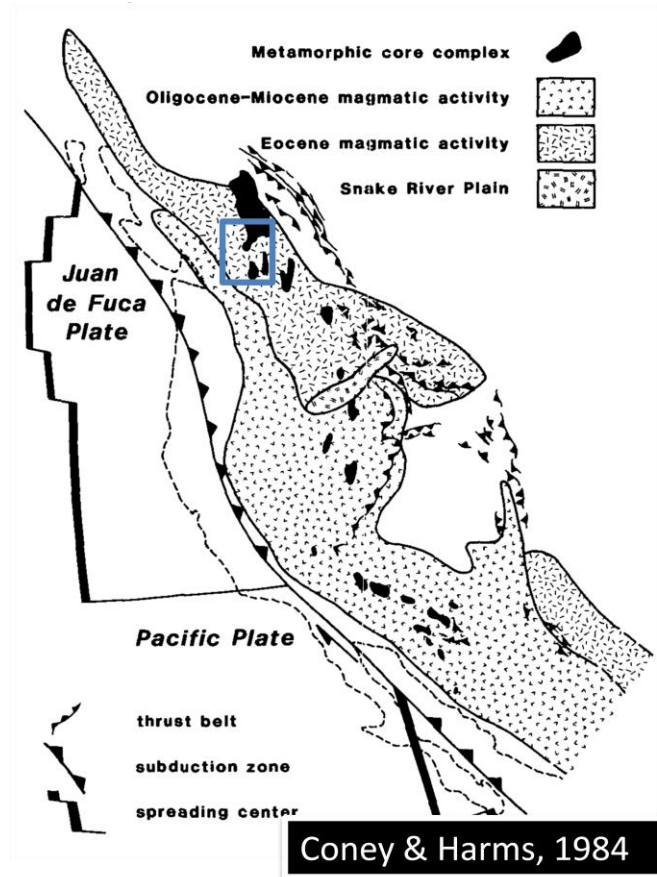


Figure 4. Metamorphic core complexes in the North American Cordillera, including the largest, the Shuswap, in British Columbia. The Okanagan study area is highlighted.

The evidence supporting the presence of a major detachment/shear zone found in this study include: a pronounced “jump” in metamorphic grade and P-T estimates across the OVSZ where the footwall is composed of upper amphibolite facies Okanagan gneiss that contain garnet-biotite schist and amphibolite while the hanging wall is composed of lower greenschist facies units, and non-metamorphosed Eocene volcanic and volcanoclastic rocks; the gently-W-dipping OVF composed of ultramylonite, cataclasite and minor pseudotachylite (e.g. Stop 1.4); and structural data including lineations and fold axes and kinematic criteria.

FIELD TRIP GUIDE

We are staying in Oliver which is located 21 km north of Osoyoos and 40 km south of Penticton on Hwy 97. Situated at the northern tip of Canada’s only desert, Oliver is the self-proclaimed wine capital of BC.

Stop 1.1 - McIntyre Bluff (viewpoint along HW97 north of Oliver)

NTS: 82E/5, **UTM:** NAD 83 11U 316190m East, 5458679m North

The cliffs of McIntyre Bluff rise 250 metres above the road. Here is our first exposure of the Okanagan gneiss; we are now within the shear zone. The Okanagan Metamorphic and Plutonic Complex has been defined as dominantly consisting of granitic orthogneiss (Parkinson, 1985) with small local occurrences of amphibolite grade paragneiss. The gneisses we will see on this trip fall into two categories based on lithostratigraphy and degree of partial melting. We interpret this section of the gneiss to be a migmatized paragneiss and orthogneiss made up of amphibolite sheets (newly dated to be ~160 Ma) that have been intruded by numerous discordant to concordant leucocratic dykes and sills (Fig. 5) including felsic pegmatites and foliated granitic bodies (peraluminous, S-type). These intrusions range in age from 98-48 Ma.

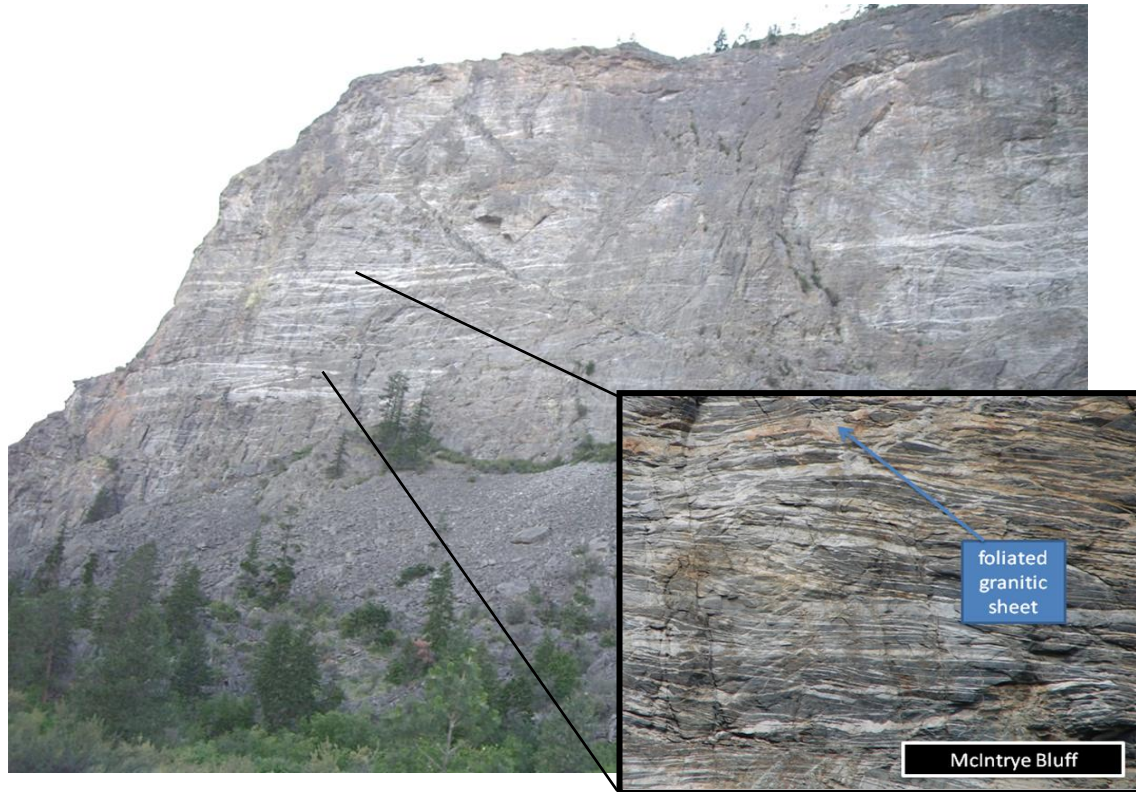


Figure 5. McIntyre Bluff viewed from the highway.

The amphibolite-grade paragneiss consists of minor schist and rare calc-silicates intruded by, and interfolded with, massive amphibolite that have been recrystallized into a biotite to hornblende plagioclase gneiss. The mineralogy of the amphibolites vary from biotite-plagioclase-hornblende to plagioclase-hornblende- with local almandine garnet. There is an intense transposed fabric with visible recumbent, sheath-like folds. Leucosomes are typically folded to the same degree as the amphibolite country rock with some later, cross-cutting felsic intrusions. In several locations there are two different generations of leucocratic layers that intruded the migmatite gneiss; a sub-horizontal set parallel to the gneissic layering cross-cuts an earlier moderately inclined set (30-45°)

The gneisses (in various works called 'Okanagan' or 'Vaseux') have some evidence of a Proterozoic history in the form of detrital cores and xenocrysts in the migmatites and intrusions. The amphibolites record a mafic intrusive event at ca. 160 Ma and later metamorphism at ~95 and 50 Ma. The intrusions contain several older cores but mainly record Eocene ages from 53-48Ma. The migmatites have a similar

age history as the intrusions. These younger ages are interpreted to represent the migmatization of the gneisses and exhumation in the Eocene.

Also note at this site we can see later stage high angle normal faults (striking to the N-NE) that cut across the outcrop (Fig. 6), formed during the late, brittle exhumation of the crystalline core along the OVF.

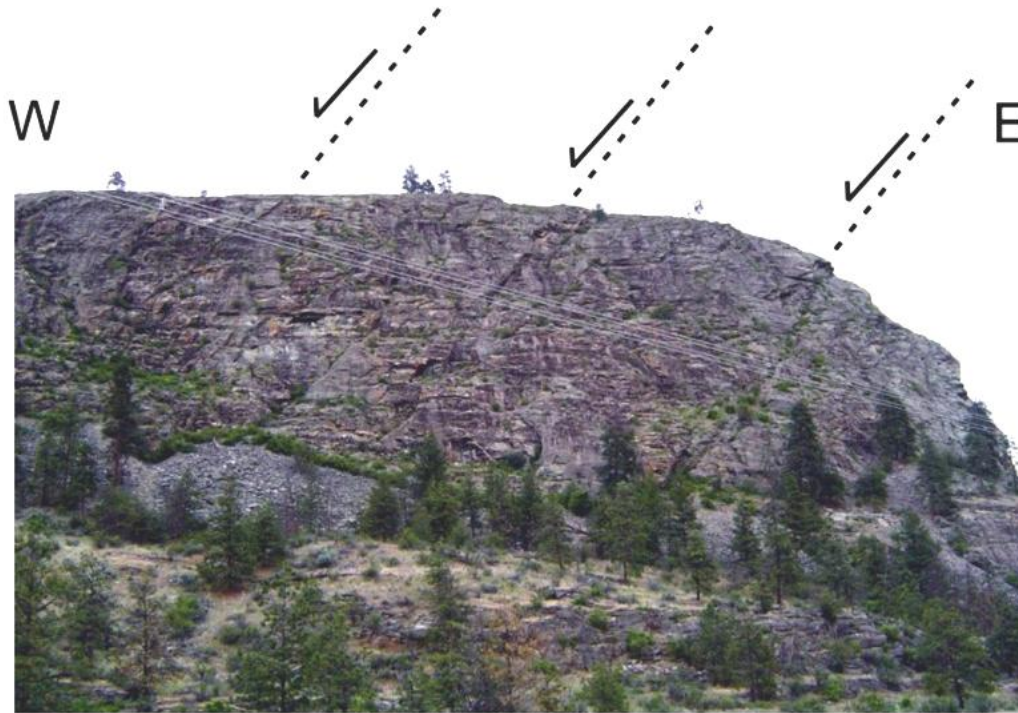


Figure 6. Stop 1.1 – view to the north from the south end of McIntyre Bluff showing late stage, west-dipping, high angle normal faults that cut the gneissic fabric.

Stop 1.2 – “Rosetta Stone” Outcrop, Highway 97

UTM: 316524 m E, 5462379 m N

Directions: Drive north along HWY 97 ~4 km to the prominent road outcrops on west side of Vaseux Lake, there is a pull-off to the left (west) of the road where you can safely park.

Key Points: close-up of the gneiss, shows cross-cutting relationships and abundant melt features (Fig. 7).

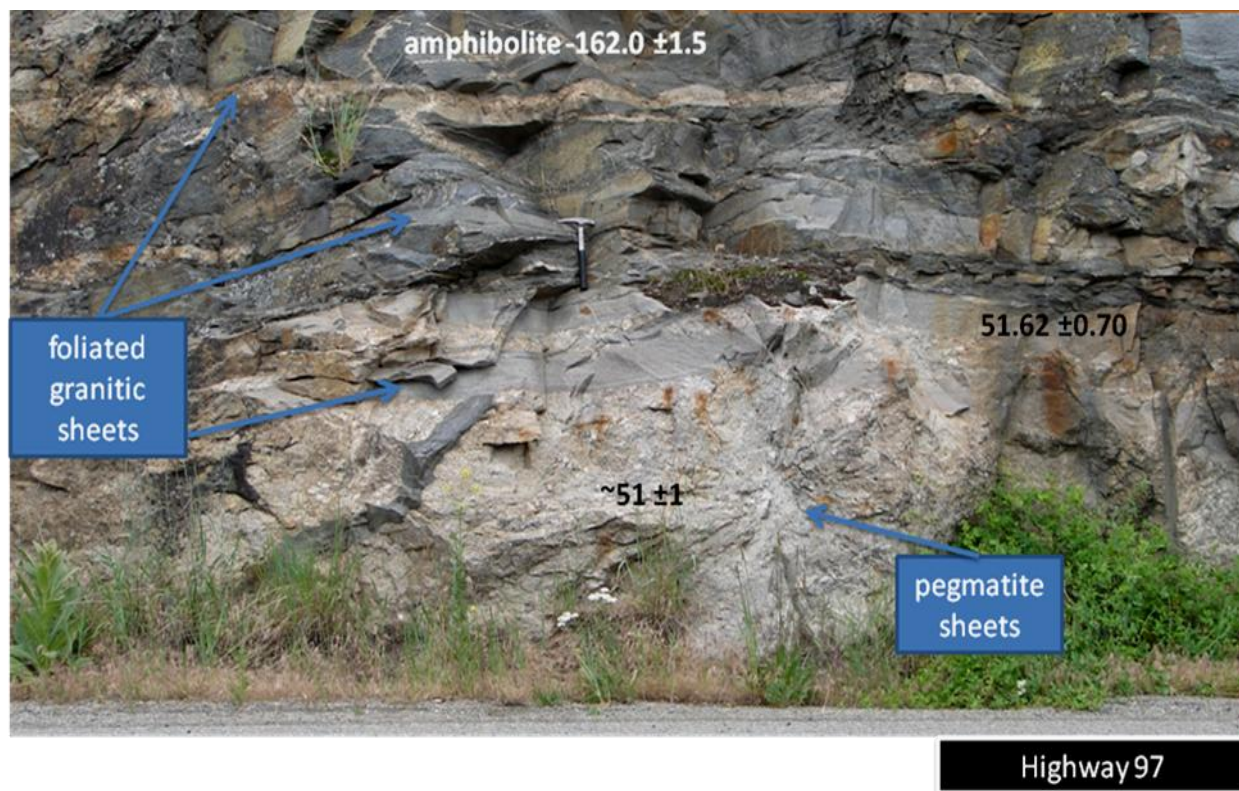


Figure 7. Stop 1.2 – “Rosetta Stone” outcrop which highlights cross-cutting relationships at Stop 1.2 that have been recently dated.

At this outcrop we can get a closer look at the migmatized amphibolite gneiss. Of note here are several gneissic granitic sheets within the outcrop. We have dated amphibolite (ca. 162 Ma), leucosome (ca. 52 Ma with several cores dating back to the Proterozoic), leucocratic pegmatite, and the biotite-bearing granite intrusions at this outcrop. While the leucosomes seem to be infolded with the amphibolite, and therefore have undergone the same late stages of deformation together, there are several syn-tectonic cross-cutting intrusions present. The medium-grained, equigranular biotite-bearing granodiorite and pegmatite give similar ages between 52 and 50 Ma (earlier events are recorded by both). While they crosscut the main transposed gneissic fabric, they are themselves foliated parallel to the gneiss (Fig. 8). We interpret them to have been injected during the last stages of extension. The pegmatites and most leucogranite sheets have muscovite, gray quartz, plagioclase, K-feldspar, almandine garnet, and chloritized biotite. A similar granite intrusion in the area gave an age of 50 Ma.

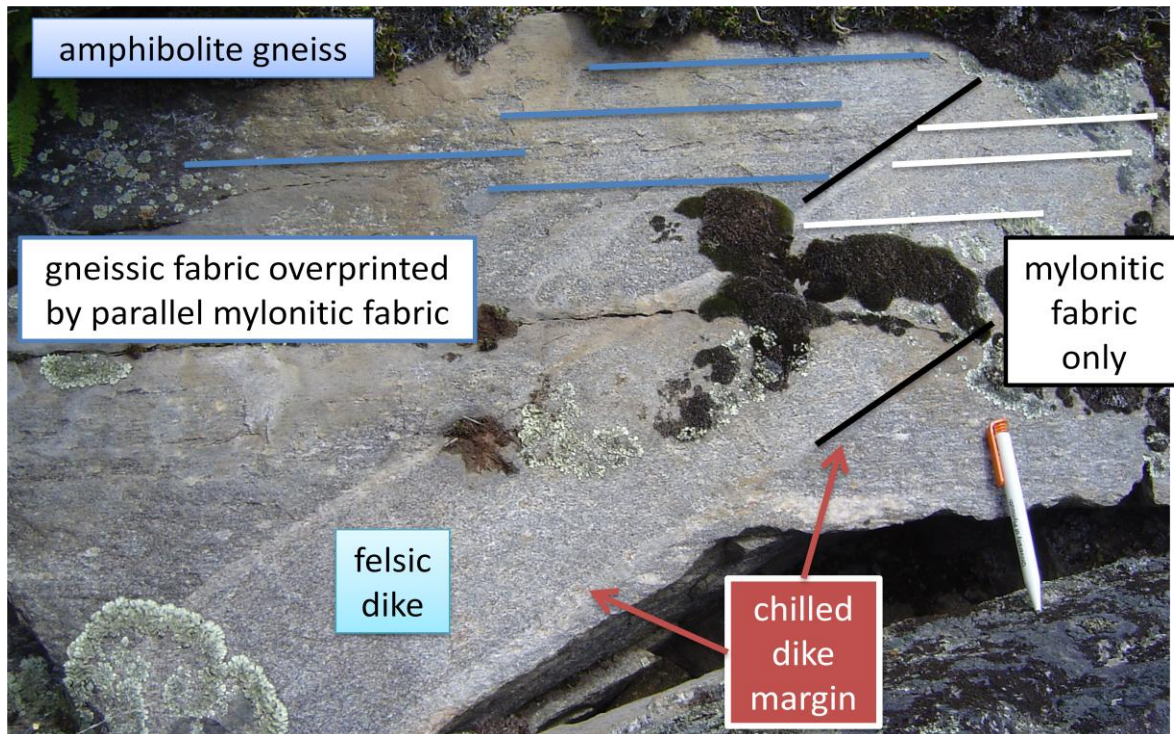
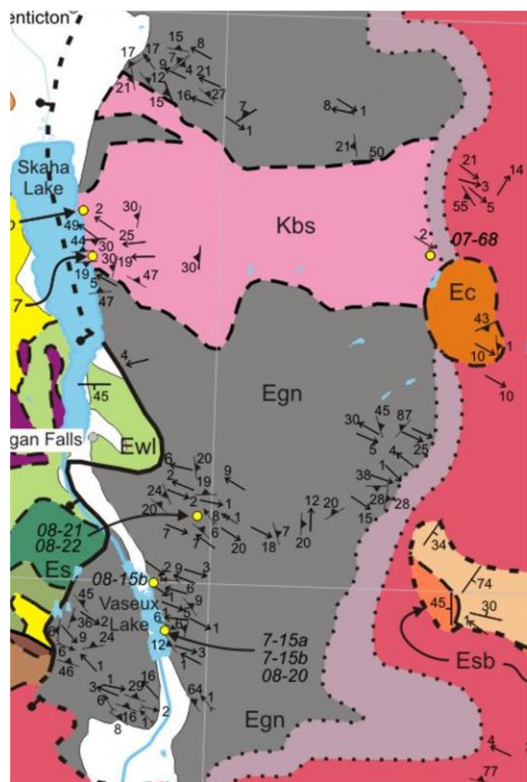


Figure 8. The intrusions *post-date* the major phase of ductile deformation in the OVSZ, but exhibit the same weak to moderate mylonitic foliation as the Okanagan gneiss implying they intruded pre- and syn-mylonitization in the OVSZ (later stages of extension).

Within the amphibolite a well developed foliation that dips WNW can be seen, which has been variably sheared to mylonitic fabrics. Structural analysis of linear fabric elements and shear sense indicators (e.g., rotated porphyroclasts, boudinaged pegmatite dykes, sheath folds, C/S fabrics) found throughout the gneisses strongly indicate extensional motion through which the hanging-wall has moved to the west. Structural information (Fig. 9) gives a dominantly NW-SE trending ($\sim 291^\circ$) stretching lineation and a nearly horizontal transposition foliation. Fold hinges interpreted to be generated during extension are generally parallel to the stretching lineation, suggesting substantial shear strain progressively rotated the fold hinges into the extensional quadrant of strain approximately parallel to the transport direction. Many fabrics have been transposed into the plane of flattening and it is often hard to find good kinematic indicators (e.g. rotated porphyroclasts) that give meaningful shear sense, but those that are discernable consistently give a tops-to-the-west-northwest sense of shear (Fig. 10).



Lineations → strong WNW-trend, plunge close to 0°. **Elongation direction WNW-ESE.**

Fold axes → gently-plunging girdle-distribution implies the dominance of sheath folds and fold axes rotation into the extension direction.

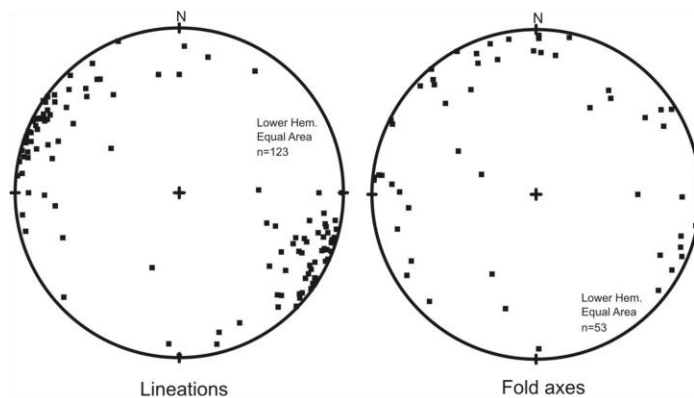


Figure 9. Structural data from the Okanagan gneiss.



consistent
top-to-the-
WNW
sense of
shear

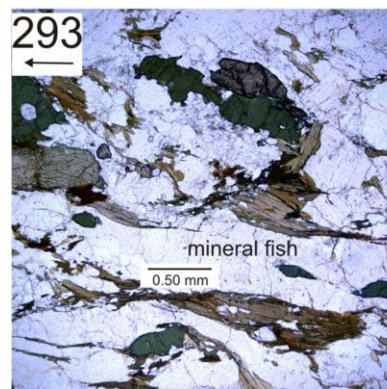
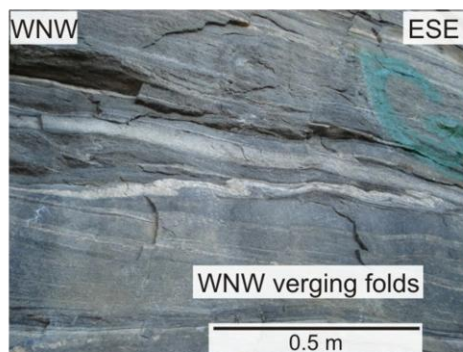
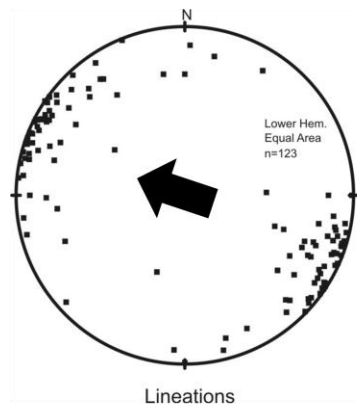
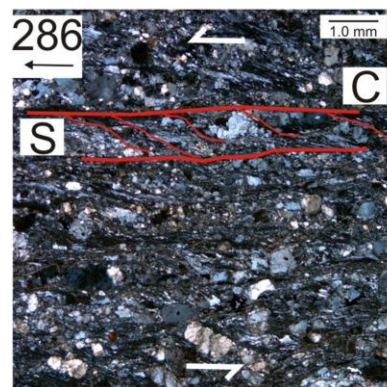


Figure 10. Some shear-sense indicators from the Okanagan gneiss showing top-down-to-the-west.

Stop 1.3 - Vaseux Lake Provincial Park Cliffs

UTM: 316150 m E, 5463991 m N

Directions: Drive north 1.7 km to Vaseux Cliffs: across from Vaseux Lake Provincial Park, just north of the park turn right onto the unmarked gravel road, park at the first bend in the road after the cattle guard.

Key points: Look at the difference in gneiss types (here it is more paragneissic), garnet-bearing pelitic rocks, transposed folds, pseudotachylyte.

This outcrop is part of the Vaseux-Bighorn National Wildlife area and care should be taken to leave as small a footprint as possible. These bluffs are part of the California Bighorn sheep habit, and also are home to several rare species of brush and reptiles. Bird watching is very popular here (Canyon Wrens, Burrowing Owls, Trumpeter Swans, Wood Ducks, Great Horned Owls, woodpeckers, Golden Eagles and Blue Winged Teals and Chukar Partridges). Be careful as there are also abundant Pacific Rattlesnakes and poison oak. *Hard hats should be worn at this site.* Climb up the boulders in the talus pile just south of the bend in the road; please proceed with caution. A pelitic assemblage should become visible where the talus pile meets the cliff; it preferentially weathers out.

Here we have amphibolite and quartzofeldspathic garnet- and biotite-bearing country rock. The quartzofeldspathic gneiss is foliated and lineated with abundant rotated porphyroclasts. This is likely a sequence of sedimentary rocks that was intruded by mafic sheets. A psammitic layer at a similar outcrop gave a few detrital ages in the Precambrian and Paleozoic, but mainly zircon crystallization ages of 50 Ma. We have dated the amphibolite sheets at ~159 Ma with metamorphism recorded at 98 and 50 Ma; a similar amphibolite gave an igneous crystallization age of 158 Ma with metamorphism recorded at 94 Ma. The amphibolite gneiss contains abundant streaks or 'stringers' of felsic material. Note the decrease in pegmatite and granite intrusions as compared to the more migmatized gneiss from the last stop. Rocks types include minor semipelite (biotite-quartz-plagioclase-garnet-muscovite) interfingering with ultramafic lenses, as well as minor calc-silicates and quartzite. The schists are within, and parallel to, the amphibolite layering. The outcrop is strongly- layered with fewer large-scale folds as compared to the migmatized version seen earlier, and have penetrative cleavage. These outcrops show mylonitic and protomylonitic fabrics and contain layers where quartz and feldspar porphyroclasts have undergone grain size reduction and the formation of pressure shadows. Throughout the section *amphibolite-facies* meta-pelites, -psammites, -quartzites, marbles, and calc-silicate layers can be found as well as *amphibolite-facies* orthogneissic amphibolite layers intercalated with meta-sedimentary layers (Fig. 11).

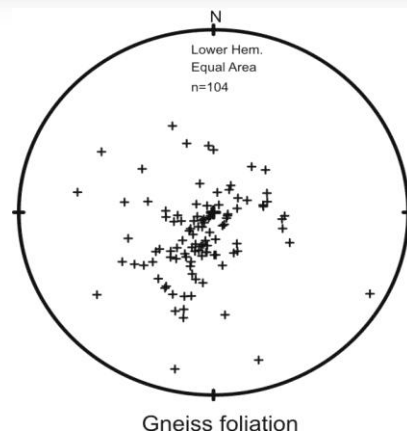


Figure 11. Transposed lithological layering in paragneiss with mylonitic fabric; foliations dip gently towards NE, N, and NW (girdle-distribution) with dips typically between 5° - 15° .

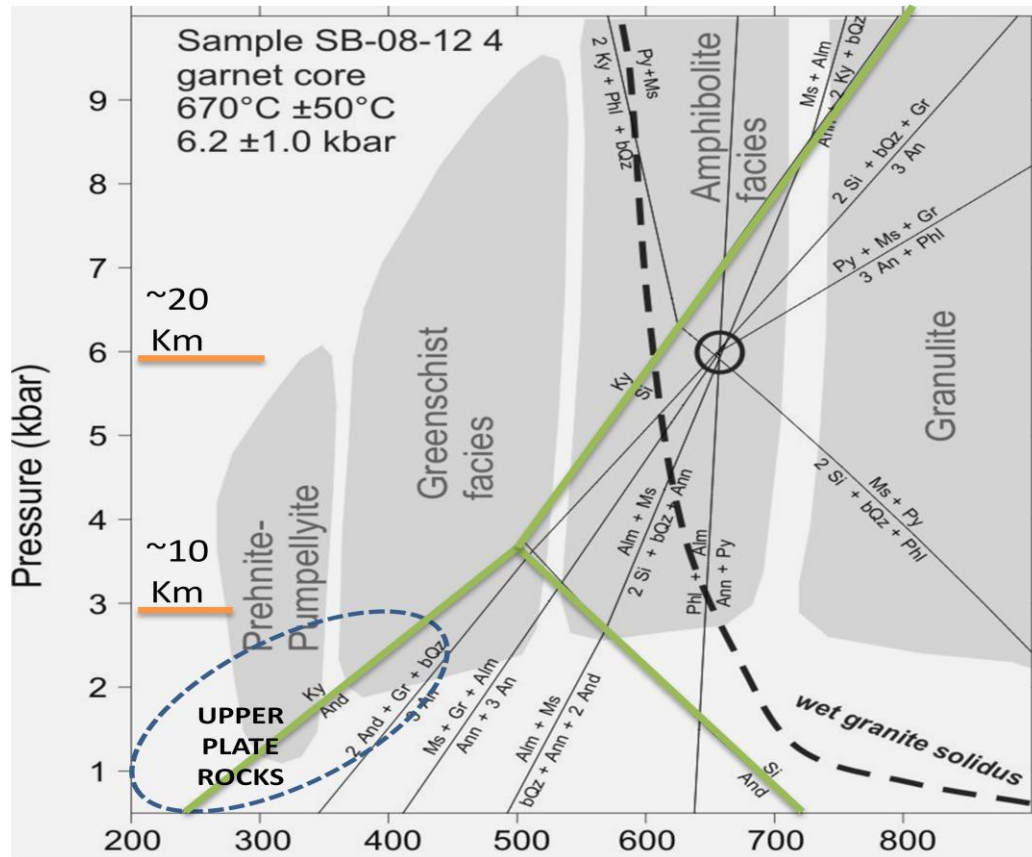


Figure 12. Pressure - Temperature plots. Analyses of garnet cores are consistent with equilibrium conditions of $670^{\circ}\text{C} \pm 50^{\circ}\text{C}$ and 6.2 ± 1.0 kbars (ca. 20 km depth). Pressures (GMAP barometer of Hoisch, 1990; 1991) and temperatures (garnet-biotite thermometer of Ferry and Spear, 1978) calculated using TWQ (v. 2.3) database of Berman (1991, 2007). Circle indicates preferred Pressure and Temperature from the reactions. Metamorphic facies appear in grey in the background as well as the wet granite solidus line. The data indicate that the pelite was reached upper amphibolite facies conditions and underwent peak metamorphism ≥ 20 km depth. Melting of hydrous rocks likely resulted in migmatite formation. P-T estimates from garnet cores & rims are nearly identical indicating no significant retrogression. This implies rapid exhumation from ~ 20 km. From Brown (2010).

After examining this area, move back down the talus pile back towards the road and follow a trail along a grassy bench north past the largest part of the rock fall. Move up the north side of the talus pile to the cliffs. There is a field of poison oak in this area so beware. There is a pseudotachylite (Fig. 11), sub-parallel to the host mylonite, which in places is up to **15 cm** thick. Flow and melt features are visible in thin section and with SEM.

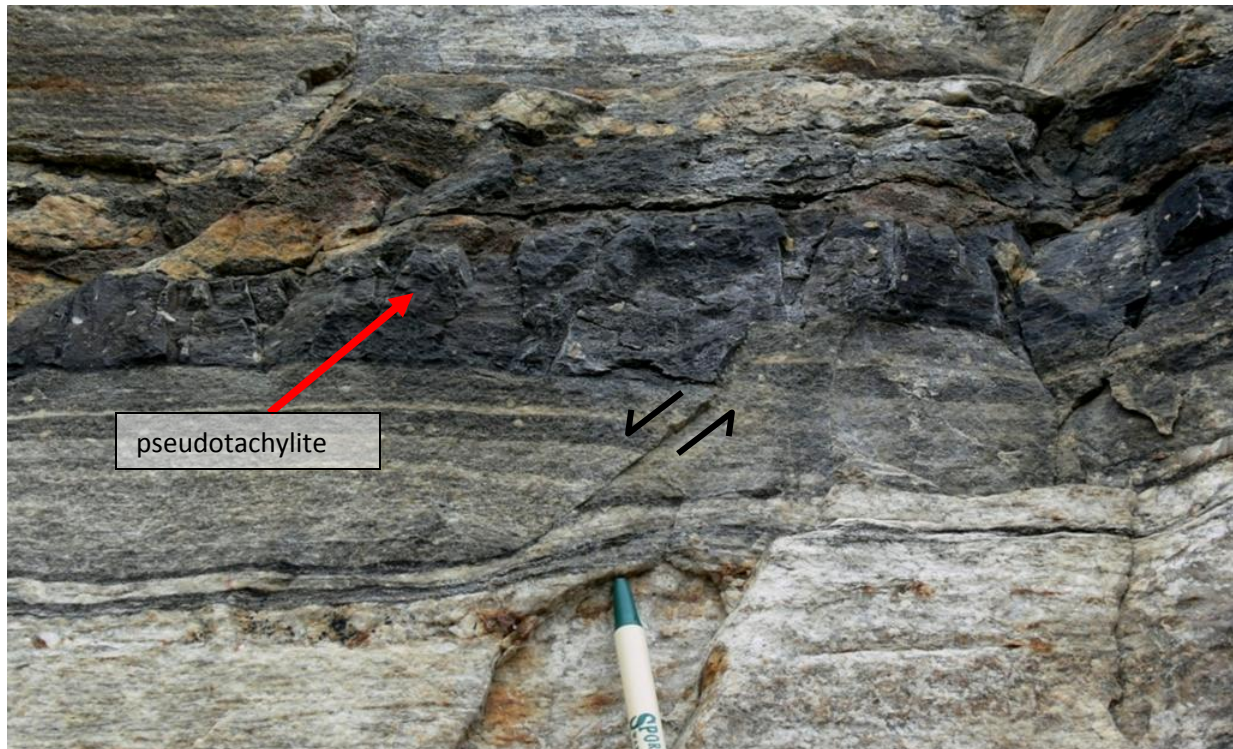


Figure 13. Stop 1.3 – view of a thick (up to 15 cm) pseudotachylite layer parallel to the gneissic fabric. The pseudotachylite contains porphyroclasts inferred to be the rounded remnants of feldspar augen from the host gneissic country rock.

Stop 1.4 - View across Vaseux Lake of footwall gneiss

UTM: 313750 m E, 5465200 m N

Directions: Drive north to Okanagan Falls, stay on HW97 until crossing bridge over Okanagan River; turn left and drive another 4 km south on Green Lake Road. Stop at top of first large switchback and view to east. (11.4 km total from Stop 1.3).

Key points: Viewing spot for footwall gneiss across valley to east

At this stop we are located on or near the trace of the brittle, upper part of the Okanagan Valley fault. The bedrock is covered by Quaternary alluvium at this location, but the purpose of the stop is to look east across the Okanagan Valley at the Vaseux gneiss. The foliation in the gneiss defines open, upright folds with northwest-trending fold axes and a wavelength of approximately 3 km (Fig. 12d). These folds are oriented similarly to broad folds in the Penticton Group (~50 Ma) on the west side of the Okanagan Valley, in the hanging wall of the Okanagan Valley fault. You are looking at one in a series of 1 – 10 km-scale, upright, WNW-trending antiformal and synformal *corrugations* parallel to the stretching direction (Fig. 13). Refer back to Figure 3 to see the corrugations at depth.

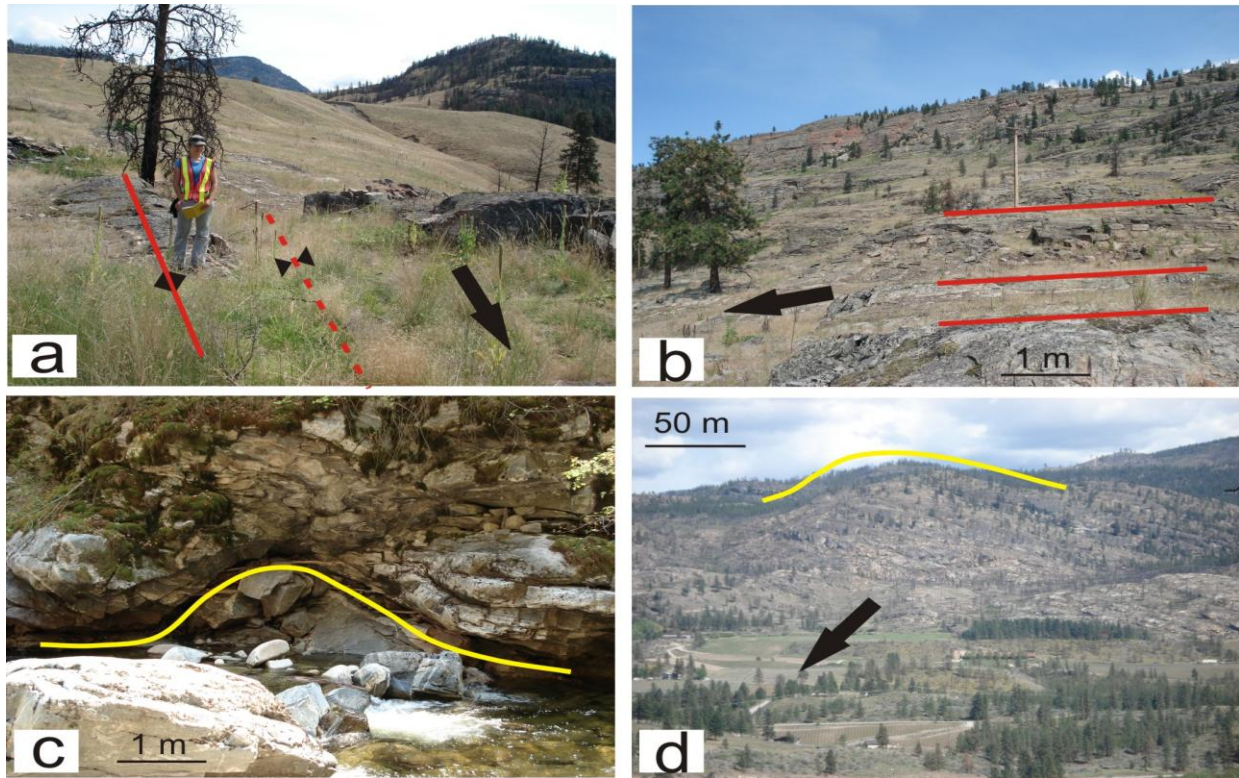


Figure 14. Field evidence of small-scale 'parasitic' corrugations. Heavy black arrow points in the direction of extensional displacement. Red lines delineate the axial surface trace of minor corrugations (a and b); yellow lines outline the profile of the corrugations (c and d).

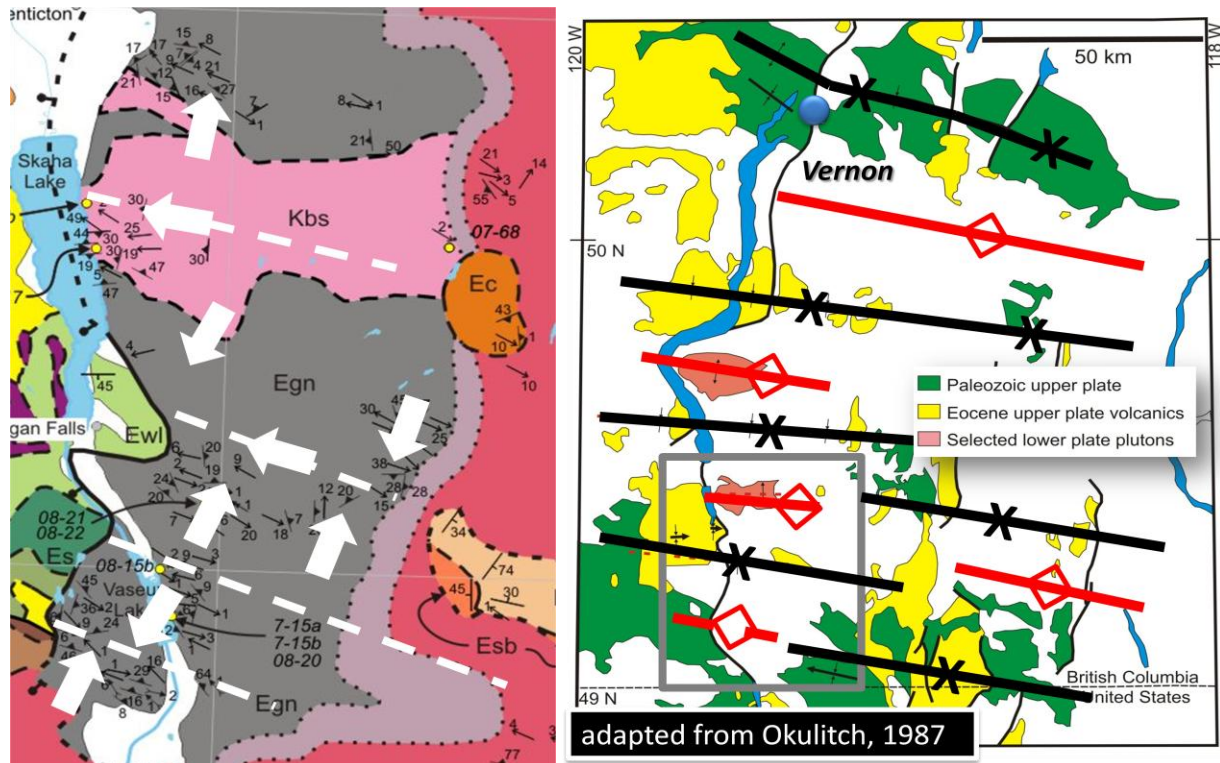


Figure 15. Corrugations defined by foliations and small upright open folds found in study area and then extrapolated throughout the region along the Okanagan Valley with mapped corrugation folds and those proposed by this study. Mapped extent of rocks typical of the upper plate of the OVSZ (yellow & green) occur in WNW-trending belts perpendicular to the OVSZ. These belts are separated by regions of granodiorite with gneissic carapaces (white & pink), typical of the lower plate. In the study area (grey box), these correspond with synformal and antiform corrugations of the OVSZ.

Corrugations appear to be present elsewhere along the OVSZ and continue south across the border. At Vernon the upper plate is continuous, i.e. there appears to be no OVSZ displacement.

Stop 1.5 - Mahoney Lake

UTM: 82 E/5 LR, 312155 m E, 5462371 m N

Directions: Drive 2.9 kilometres south on the Green Lake Road and park in pull out on east side of road

Key points: Walk along trace of OVF, examining hanging wall volcanics juxtaposed next to footwall gneisses; both show varying degrees of alteration attributed to fluids associated with the OVF

Mahoney Lake is in an ecological reserve and exhibits a transition area from altered volcanic and sedimentary rocks to cataclases, ultramylonites and amphibolite. Mahoney Lake is 18 metres deep and occupies a glacially formed kettle depression. The underlying bedrock of fractured lava has a highly alkaline composition which results in water that has very low oxygen levels and is very high in salinity and alkalinity. Mahoney Lake is on the world registry of meromictic (non-mixing) lakes and is recognized in the international limnological literature as one of the outstanding meromictic lakes in the world.

The upper, brittle part of the Okanagan Valley fault runs through Mahoney Lake with volcanic and coarse clastic rocks to the west and gneiss to the east. Adjacent and structurally down-section from the brittle

fault, the gneiss is altered, largely to chlorite and pyrite. Parts of the gneiss are strongly mylonitic. Chloritization is at least partly synchronous with the youngest mylonitization, as indicated by deformed chlorite in the mylonite. The rocks grade structurally upward from mylonite/ultramylonite into microfractured mylonite, brecciated mylonite to brecciated, chloritized and silicified upper plate rocks. In places the mylonites have 'relict' banded texture (see Fig. 14).

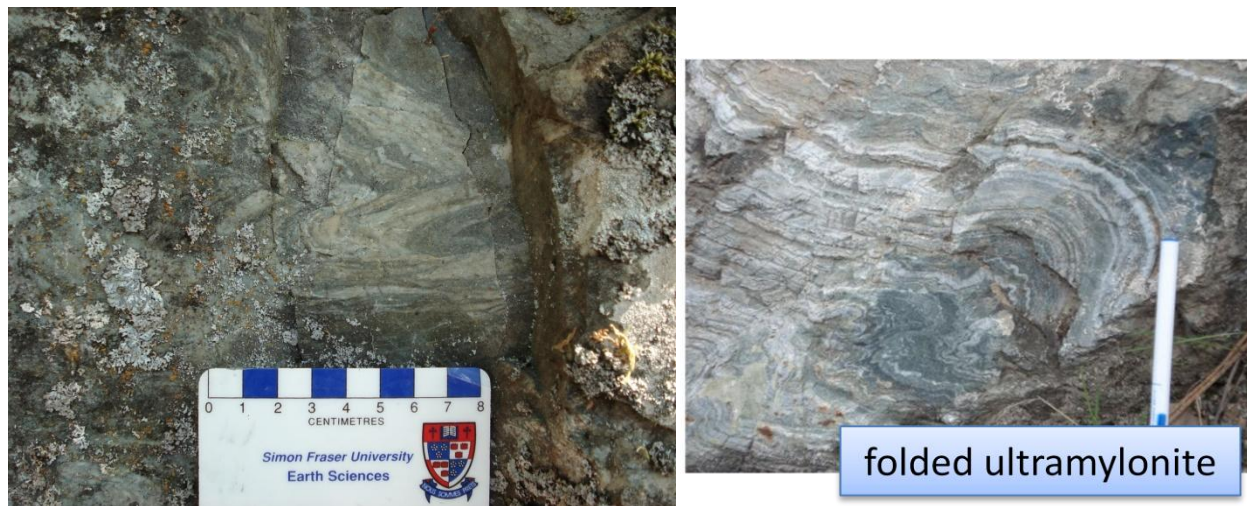


Figure 16. Stop 1.5 - Silicified banded mylonite at Mahoney Lake.

There is a strong brittle overprint emplaced on the ductile textures (Fig. 15) in the mylonite, presumably reflecting the brittle overprint on the ductile shear zone as it was exhumed through the upper crust. Broad, upright crenulations and folds can be found in a few areas but mainly tight, isoclinal, recumbent folds dominant the gneiss and mylonite.



Figure 17. Cataclastic overprint of the mylonitic fabric.

We can see conglomerate on the roadway NE of the N end of Mahoney Lake, and altered volcanics at the pull-off on the S end of Mahoney Lake. The volcanics are altered and contain limonite.

Concluding Remarks

This field guide is the result of a PhD study (under Drs. Dan Gibson & Derek Thorkelson) that reconfirmed there is a major break in metamorphic grade across the region (with equilibration at 20 km depth), there is a low-angle detachment fault exposed along the Okanagan Valley (the OVF) and that the Okanagan gneiss forms the dominant part of a major fossilized ductile shear zone (the OVSZ). The OVSZ dips $\sim 15^\circ - 30^\circ$ to the WNW, shows E-W extension, with transport *top-to-the-WNW*, contains transposed layering, sheath folds, mylonitic fabric, and is folded into WNW-trending corrugations and synclinal corrugations that appear to be zones of little or no extension.

The amphibolite layers in the paragneiss are interpreted to be igneous intrusions that were emplaced between 162-157 Ma, therefore they must post-date deposition of sedimentary country-rock (paragneiss) putting a upper age limit on the sedimentary country rock. The amphibolite layers also show evidence for high-temperature metamorphism (including zircon growth) during the Cretaceous (98-93 Ma) and Eocene (50 Ma), which is in line with what is known about the geologic history of the region, Cretaceous – peak Cordilleran orogeny and metamorphism and Eocene – exhumation.

Felsic leucosomes within the Okanagan gneiss are infolded and transposed with the paragneiss and amphibolite layers; they record 53-50 Ma *migmatization* (melting) during high-temperature metamorphism and xenocrystic cores give ages ranging from the Proterozoic to Early Jurassic (inferred to come from melted country-rocks).

The late syn-deformation dikes and sills contain magmatic euhedral zircon crystals and ims that give U-Pb ages of **53 – 49 Ma** (Eocene).

	<i>lithology</i>	<i>interpretation</i>
Paragneiss domain	amphibolite-facies meta-pelites, - psammites, - quartzites, marbles, and calc-silicate layers	\geq Late Jurassic marine sedimentary sequence (probably composed of turbidites) \rightarrow includes Proterozoic - Early Jurassic xenocrystic zircons.
	amphibolite-facies orthogneissic amphibolite layers intercalated with meta-sedimentary layers	~ 160 Ma (Late Jurassic) mafic -intermediate sills and dikes intruded into sedimentary succession \rightarrow geochemistry suggests a paired oceanic arc-back-arc system.
Orthogneiss domain	intensely- to weakly-foliated granodiorite (gradational with non-deformed granodiorite)	Late Jurassic to Eocene granodiorite plutons (Okanagan batholith) deformed within the Okanagan Valley shear zone.

Table 2. Gneiss protolith chart. The Okanagan gneiss was developed primarily in the Eocene through deformation and metamorphism of sedimentary and igneous rocks within the OVSZ. Exhumed along the OVF, the orthogneiss was derived from the shearing of Mesozoic and Eocene plutons in the footwall, and

the paragneiss domain was derived from a combination of sedimentary units in a marine setting and subsequently intruded by Jurassic mafic sills and dikes.

Exhumation of the Okanagan gneiss from ~20 km along a 15°– 30° WNW-dipping, 1.5 – 2 km wide ductile shear zone from 53-49 Ma equates to 29 – 86 km of E-W extension. Identification of corrugation folds of the OVSZ can explain the apparent absence of a major detachment along strike, e.g., in the Vernon area.

References

- Armstrong, R., 1982, Cordilleran metamorphic core complexes – from Arizona to southern Canada. *Annual Reviews of Earth Planetary Science*, v. 10, p. 129-154.
- Bardoux, M., 1993, The Okanagan Valley normal fault from Penticton to Enderby--South-central British Columbia. Ph.D. thesis: Carleton University, Ottawa, Ontario, 292 p.
- Berman, R.G. ,1991, Thermobarometry using multi-equilibrium calculations: a new technique, with petrological applications. *In* Quantitative methods in petrology: an issue in honor of Hugh J. Greenwood. *Edited by* T.M. Gordon and R.F. Martin. *Canadian Mineralogist*, v. 29, p. 833-855.
- Berman, R.G. 2007. winTWQ (version 2.3): a software package for performing internally-consistent thermobarometric calculations. Geological Survey of Canada, Open File 5462, (ed. 2.34), 41 p.
- Brown, R. L., Gibson, H.D., 2006, An argument for channel flow in the southern Canadian Cordillera and comparison with Himalayan tectonics, *in* Law R. R., Searle, M.P., Godin, L., eds, Channel flow, ductile extrusion and exhumation in continental collision zones, Geological Society London Special Publication 268, p. 543-559.
- Brown, S. R., 2010, Geology and geochronology of the southern Okanagan Valley shear zone, southern Canadian Cordillera, British Columbia. Ph.D. thesis: Simon Fraser University, Burnaby, British Columbia, 332 p.
- Cook, F. A., Varsek, J.L., Clowes, R.M., Kanasewich, E.R., Spencer, C.S., Parrish, R.R., Brown, R.L., Carr, S.D., Johnson, B.J., Price, R.A., 1992, Lithoprobe crustal reflection cross section of the southern Canadian Cordillera, 1. Foreland thrust and fold belt to Fraser River Fault, *Tectonics*, v. 11, p. 12-35.
- Cook, F. A., 1995, The reflection Moho beneath the southern Canadian Cordillera. *Canadian Journal of Earth Sciences*, v. 32, 1520-1530.
- Coney, P., 1980, Cordilleran metamorphic core complexes: An overview, *in* Crittenden, M., Coney, P., and Davis, G., eds, Cordilleran metamorphic core complexes. Geological Society of America Memoir, v. 153, p. 7-34.
- Coney, P., Harms, T., 1984, Cordilleran metamorphic core complexes: Cenozoic extensional relics of Mesozoic compression. *Geology*, v. 12, p. 550-554.
- Ferry, J.M., Spear, F.S., 1978, Experimental calibration of the partitioning of Fe and Mg between biotite and garnet. *Contributions to Mineralogy and Petrology*, v. 66, p. 113-117.
- Glombick, P. 2005. Mesozoic to early Tertiary tectonic evolution of the Shuswap metamorphic complex in the Vernon area, southeastern Canadian Cordillera. Unpublished Ph.D. thesis, University of Alberta, Edmonton, Alberta.
- Glombick, P., Thompson, R., Erdmer, P., Daughtry, K., 2006, A reappraisal of the tectonic significance of early Tertiary low-angle shear zones exposed in the Vernon map area (82 L), Shuswap metamorphic complex, southeastern Canadian Cordillera: *Canadian Journal of Earth Sciences*, v.43, p. 245-268.
- Glombick, P., Thompson, R.I., Daughtry, K.L. 2004, Geology of the Oyama map area, British Columbia (NTS 82 L/03). Geological Survey of Canada, Open File 4372, scale 1:50 000.
- Hoisch, T.D. 1990, Empirical calibration of six geobarometers for the mineral assemblage quartz + muscovite + biotite + plagioclase + garnet. *Contributions to Mineralogy and Petrology*, v. 104, p. 225–234.
- Hoisch, T.D., 1991, Equilibria within the mineral assemblage quartz + muscovite + biotite + garnet + plagioclase, and implications for the mixing properties of octahedrally-coordinated cations in muscovite and biotite. *Contributions to Mineralogy and Petrology*, v. 108, p. 43–54.
- Johnson, B.J., 1994, Structure and tectonic setting of the Okanagan Valley fault system in the Shuswap Lake area, southern British Columbia. Unpublished PhD Thesis, Carleton University, Ottawa, Ontario, Canada.
- Johnson, B.J., Brown, R.L., 1996, Crustal structure and early Tertiary extensional tectonics of the Omineca belt at 51°N latitude, southern Canadian Cordillera, *Canadian Journal of Earth Sciences*, v. 33, p. 1596-1611.

- Johnson, B.J., 2006, Extensional shear zones, granitic melts, and linkage of overstepping normal faults bounding the Shuswap metamorphic core complex, British Columbia, GSA Bulletin, v. 118, p. 366-382.
- Kruckenberg, S.C., Whitney, D.L., Teyssier, C., Fanning, C.M., and Dunlap, W.J. 2008. Paleocene-Eocene migmatite crystallization, extension, and exhumation in the hinterland of the northern Cordillera: Okanogan dome, Washington, USA. Geological Society of America Bulletin, v. 120, p. 912-929.
- Monger, J., Price, R., Tempelman-Kluit, D., 1982. Tectonic accretion and the origin of two major metamorphic and plutonic belts in the Canadian Cordillera. Geology, v. 10, p.70-75.
- Okulitch, A., 1979. Geology and mineral occurrences of the Thompson-Shuswap-Okanagan region, south-central British Columbia: Geological Survey of Canada Open File 637, scale 1:250,000, 3 sheets.
- Okulitch, A.V. 1987. Comment on "Extension across the Eocene Okanagan crustal shear in southern British Columbia." Geology, **15**: 187-188.
- Parkinson, D., 1985. U-Pb geochronology and regional geology of the southern Okanagan Valley, British Columbia: The western boundary of a metamorphic core complex. Unpublished M.S. thesis, University of British Columbia, Vancouver, British Columbia, 149 p.
- Parrish, R. R., Carr, S. D. Parkinson, D. L., 1988. Eocene extensional tectonics and geochronology of the southern Omineca Belt, British Columbia and Washington. Tectonics, 7, 181–212.
- Spencer, J.E., Reynolds, S.J. 1989, Tertiary structure, stratigraphy, and tectonics of the Buckskin Mountains. *In* Geology and mineral resources of the Buckskin and Rawhide Mountains, west-central Arizona. *Edited by* J.E. Spencer and S.J. Reynolds. Arizona Geological Survey Bulletin, 198: 103–167.
- Tempelman-Kluit, D., Parkinson, D., 1986. Extension across the Eocene Okanagan crustal shear in southern British Columbia: Geology, v. 14, p. 318-321.
- Tempelman-Kluit, D.J. 1989: Geology, Penticton, British Columbia; Geological Survey of Canada, Map 1736A scale 1: 250 000.
- Thompson, R.I., Unterschultz, J.L.E. 2004. Geology of the Vernon map area, British Columbia (NTS 82 L/06). Geological Survey of Canada, Open File 4375, scale 1:50 000.

CTG 30th Annual Meeting- Presentation Schedule
Venue: The Discovery Room

9:00 – 9:20: Félix Gervais, Andrew Hynes, Edward D. Ghent

The Hellroar Creek Shear Zone: A Major Tectonic Boundary In The Northern Monashee Mountains Of The Southeastern Canadian Cordillera

9:20 – 9:40: Jenny Haywood And Lori Kennedy.

Mechanical Constraints On Carbonate And Shale Composite Fault Gouges: Implications For Natural Faults

9:40 – 10:00: Joe White

Mechanical Amorphization During Experimental Shearing Of Synthetic Granite

10:00 – 11:00 COFFEE BREAK AND POSTERS.

11:00 - 11:20: Stephan Kolzenburg, Yan Lavalée, Ulrich Küppers, Kelly Russell, Lori Kennedy

Tuffites: circling the rheological glass transition

11:20-11:40: Laurent Godin, Chris Yakymchuk, Lyal B. Harris

Himalayan Hinterland-Verging Superstructure Folds Related To Foreland-Directed Infrastructure Ductile Flow: Insights From Centrifuge Analogue Modelling

11:40 – 12:00: Prince Amponsah

Multiscale Structural Analysis Of The Sunyani Basin, Ghana

12:00 – 2:00 LUNCH AND POSTERS

2:00 – 2:20: C. Willem Langenberg And Tijmen (Tim) H.D. Hartel

Fracture Analysis And Use Of Lidar, Turtle Mountain, Alberta

2:20 – 2:40: B.A. Friedlander, L.A. Kennedy, J.K. Russell, J. Pallister

Mechanisms Of Strain Localization Within The 2004-2008 Mt. St. Helens Lava Domes: The Role Of Effusion Rate?

2:40-3:00. Kennedy, Lori A., Russell, Kelly

Ash Production Through Brittle Cataclasis During Dome Emplacement

3:00 – 3:20: Greg Sinitsin

Wave Theory And Tectonics

Fracture analysis and use of LiDAR, Turtle Mountain, Alberta

C. Willem Langenberg and Tijmen (Tim) H.D. Hartel
Long Mountain Research Inc., Edmonton and Rock Proof Ltd., Calgary
cwlangen@telus.net and timprove@yahoo.com

The rocks of the Turtle Mountain area are intensely fractured. The Paleozoic carbonates are of most interest regarding the structure of the mountain. The Paleozoic carbonates are folded into a large anticline (the Turtle Mountain Anticline) with a steeply dipping to overturned east limb that lies above a fault (the Turtle Mountain Thrust). The timing of movements along this fault is unknown. Movements probably started in the Paleocene and might still continue today, as indicated by small local seismic events along the fault observed by the Turtle Mountain microseismic system (Chen *et al.*, 2005). The main movements might have been around 52 Ma in the early Eocene (van der Pluijm *et al.*, 2006).

Fracture fabrics of these carbonates were measured in outcrop, obtained from image logs in a borehole and from slope analysis. The majority of fractures are extensional fractures with accompanying shear fractures related to the main anticlinal fold. The three most frequent orientations seen are the northwest-dipping steeper-than-bedding set, the set dipping steeply northeast sub-parallel to the Frank Slide surface (“scary” joints) and the set that dips ~30° southeast toward Hillcrest. The “scary” fractures are also found in Palliser breccia immediately above the thrust faults. Fractures observed in the borehole show comparable orientations.

These fracture orientations were compared with the orientations obtained from slope analyses. These slopes were determined from detailed DEM's obtained from LiDAR data. These investigations identified six fracture sets influencing the slope instability and surface morphology. Three fracture sets (sets J2, J3 and J4) have a fixed relation with the fold axis direction and are correlated with the folding/thrusting phase during Paleocene/Eocene. The other fracture sets (J1, J5 and J6) are possibly post-folding resulting from unloading movements during Miocene to the present. Stress release during this relaxation period has likely played a role in reactivation of syn-folding structures, such as J2 and J3.

References

Chen, Z., Stewart, R.R. and Bland, H.C. (2005): Analysis of microseismicity at a mountain site; CREWES Research Report, University of Calgary, v.17, chap. 7, p. 1-28.

van der Pluijm, B.A., Vrolijk, P.J., Pevear, D.R., Hall, C.M., and Solum, J.G. (2006): Fault dating in the Canadian Rocky Mountains: evidence for late Cretaceous and early Eocene orogenic pulses; *Geology*, v. 34, p. 837-840.

Mechanical amorphization during experimental shearing of synthetic granite gouge

Joseph Clancy White

Department of Geology, University of New Brunswick, Fredericton NB E3B 5A3
email: clancy@unb.ca

Frictional sliding experiments performed in a rotary shear machine at 25 MPa normal stress on 2-mm thick layers of simulated Westerly granite gouge (initial particle size 1-85 μm) have produced heterogeneous microstructures comprising comminuted material with internal layering. In SEM/BSE individual layers comprise grains of rounded and sub-rounded quartz and feldspar particles that vary in size from 20nm on one side to about 300nm on the other. Characterization of the gouge ultrastructure has been undertaken by analytical scanning transmission electron microscopy (STEM). Areas were selected from high-magnification SEM images and thinned in a focused ion beam instrument (FIB). This sampling procedure produces material of even electron transparency with perfect spatial registration to the optical and SEM microstructures. The sub-micrometre-scale laminar variation of grain size and porosity is confirmed by STEM. Shards of both feldspar and quartz are progressively comminuted to form the texture in which larger grains are surrounded by finer-communited matrix material. Grains of both of the latter primary mineral constituents are routinely less than 100 nm in size. Most significantly, the finest grained, least porous zones comprise small grain fragments embedded within an amorphous silicate matrix. By extension, one can infer that observation of these zones throughout the gouge is consistent with extensive amorphization during the shearing. The internal layering of the brecciated fragments, with asymmetric particle size and porosity grading, indicates that Y-slip surfaces localize displacement until particles that line the slip surface are reduced to a critical size that enables mechanically induced amorphization. Fluctuations in friction recorded during formation of this microstructure can be reasonably related to cyclic softening-hardening related to porosity loss and amorphization, with subsequent brecciation of the gouge during slip on multiple Y-slip surfaces.

Wave Theory and Tectonics

by Greg Sinitsin, Global Impact Exploration ,Vernon B.C.

ABSTACT:

Major topographical variance on the Earth (i.e. oceans and continents) can be explained using “wave” theory. Mountain ranges are the “crest” of a wave that is moving around the circumference of the Earth propelled by the tidal forces. The wave “crests” forms the continents, while the wave “troughs” form ocean basins – or geosynclines. The tidal forces propel these waves. Mountain ranges exhibited wave-like properties particularly the Rocky Mountains.

Gravity drag from the Sun and Moon pulls on the Earth to deform its shape (evidenced by ocean tides) while, at the same time, the spinning sphere acts to maintain its equilibrium (isostasy). The stresses from these competing forces are relieved in the form of waves that move through Earth’s crust; these waves elevate or depress the Earth’s crust and form the continents and ocean basins.

The antipodal location of the continents and oceans along with the triangular shape of the continents support this hypothesis. One example supporting the Plate Tectonics theory is terrane accretion or stacking and is refuted in this paper

GEOLOGY OF THE OKANAGAN WATERSHED, SOUTH-CENTRAL BRITISH COLUMBIA

1. [OKULITCH, Andrew V.](#), Natural Resources Canada, Geological Survey of Canada, 625 Robson Street, Vancouver, BC V6B 5J3 Canada, aokulitc@nrcan.gc.ca

The geology of the map-area was compiled from maps at scales of 1:250 000 to 1:10 000 spanning 70 years. Concepts that influenced interpretation of field data evolved considerably over that time. Integration of the diverse maps was challenging; not all elements were resolved. The process was a cautionary reminder of the limitations that bias, model-driven interpretations and changing concepts impose on geological research.

In Canada, the watershed extends north from the 49th parallel for 180 km along the western margins of the Shuswap and Okanagan Metamorphic and Plutonic complexes and east-west 100 km at its widest part. High grade rocks predominantly in the eastern half of the watershed are poorly dated but may include strata of Paleozoic age intruded by Mesozoic and Paleogene granitic rocks. Low grade rocks in the western half range in age from Ordovician to Quaternary but are mostly Carboniferous to Triassic and Eocene. These are assigned to Quesnel Terrane and its overlap assemblages, except those in the northernmost part of the watershed which have been suggested to have affinities with peri-cratonic North American successions. Accretion of Quesnel Terrane to North America began during the Permo-Triassic and continued into the Jurassic and Cretaceous accompanied by extensive magmatism.

The main valley was initially interpreted to contain steep normal faults. Later, mylonite zones and kinematic indicators suggested that a gently west-dipping, top-to-the-west detachment fault with displacement as much as 100 km affected Eocene and older strata. K/Ar dates indicating an Eocene thermal event restricted to the complexes were reinterpreted to date the denudation. Eocene strata dipped at all angles to the detachment.

More recently, some mylonite zones were dated as Mesozoic and some contacts between low and high grade rocks were interpreted to be depositional. Major stratigraphic belts were mapped across the valley in the northern part of the watershed. Eocene volcanics were observed in apparent stratigraphic contact with high grade rocks as well as against steep normal faults. No simple, continuous detachment was evident. In several instances, low-angle faults diverged markedly from the valley.

Such differing interpretations can be resolved in a complex model involving multiple, non-planar, polyphase detachments. In the complexes one or more episodes of deformation and metamorphism predate Eocene faulting and the ages of many of these events and the metamorphic protoliths are unknown. In low grade rocks deformation occurred from the Permo-Triassic to Paleogene and any pre-denudation deformation might be expected to have affected underlying rocks. Transitions between low and high grade rocks occur east and west of the valley. Most are abrupt and clearly faulted and their distribution can be explained by one detachment gently warped about approximate east-west axes. In addition, detachment may have occurred at more than one structural. Several discontinuous detachment faults may die away northward into a zone of normal faults and/or descend into high grade rocks east of the valley. Mylonite and brittle fault zones accompanied by extensive hydrothermal systems, formed before, during and after a prolonged episode of Eocene volcanism.

The bedrock relief of the watershed exceeds that of the Grand Canyon of the Colorado and has been suggested to have contributed to the glacial-age floods of the Channeled Scablands.

Tuffisites: circling the rheological glass transition

Stephan Kolzenburg¹, Yan Lavalée², Ulrich Küppers², Kelly Russell¹, Lori Kennedy¹

1: University of British Columbia; Department of Earth and Ocean Sciences

2: Ludwig-Maximilians-University, Munich; Department of Earth and Environmental Sciences

On the ascent path towards the Earth's surface magmas may undergo brittle failure by crossing the rheological glass transition. Extrusion speeds that exceed the relaxation timescale of a melt create shear-induced-stress that, when reaching the yield strength of the magma, results in fragmentation of the magma. Magmatic gases released during ascent use these fractures as pathways to vent to the atmosphere and reduce volcanic overpressures. However, The fragmentation products created by these events can anneal or weld if they are maintained above their glass transition temperature long enough to relax viscously.

Tuffisites (Fig. 1) are veins and sheets of pyroclastic material created during such events. They occur in and around volcanic conduits. Very little modern research has been carried out on this type of deposit despite the fact that their characteristics can be used to improve and test current ideas on fracture processes within magma, gas escape and the interaction of the gas- and melt phase during eruptions.



Figure 1: Sample of obsidian lava flow from Lipari, Italy displaying tuffisite veins (grey) having different degrees of sorting (i.e. clast sizes). G denotes the massive unfragmented quenched magma (i.e. glass); F denotes the clastic layers resulting from fragmentation of that magma (i.e. tuffisite).

Here I give an insight to textures of Tuffisites found in an explosion breccia near the vent of an Obsidian flow on the north east shore of the island of Lipari, Italy.

Further I present observations on the deformation behaviour of these rocks derived from uniaxial, high temperature rock deformation experiments.

In microscopic analysis the Tuffisite veins reveal a multistage formation process. Macroscopic veins are composed of a number of re-welded layers that vary in grainsize distribution and sorting, suggesting differences in their emplacement mechanism.

Mechanical constraints on carbonate and shale composite fault gouges: Implications for natural faults

Jenny Haywood and L.A. Kennedy
University of British Columbia

Carbonate and phyllosilicate-rich fault gouges are common in fault zones worldwide. Despite numerous and diverse examples of shale and carbonate -rich fault zones (e.g. fold and thrust belts, such as the foreland of the Canadian Rockies, the Glarus thrust, Switzerland, the Appalachians, USA; and strike-slip faults, e.g. the San Andreas, USA and the Carboneras Fault Zone, Spain) little is known about the rheological behavior of these composites.

We report on the results of velocity-stepping frictional sliding experiments conducted on carbonate and shale composites. We examine the effect of gouge composition and forcing block porosity on the strength, stability, fabric and microstructural evolution of calcite and shale gouge zones.

Room temperature, triaxial frictional sliding experiments were conducted on 2.54 mm diameter by 50 mm length cores containing a 1 mm thick, water saturated gouge layer along a 35° angle sawcut. Experiments were performed on each endmember composition as well as 75%, 50% and 25% mixtures of shale and carbonate. In one suite of experiments, porous Berea Sandstone ($\phi \sim 17\%$) comprised the upper forcing block while impermeable Badshot Dolomite comprised the lower forcing block. In a second suite, Badshot Dolomite comprised both forcing blocks. Experiments were conducted at 70 MPa confining pressure and displacement rates varied between 10^0 to $10^2 \mu\text{m s}^{-1}$.

All gouge compositions show velocity dependency at the conditions tested. 100% carbonate gouge exhibits velocity weakening behavior under some conditions, but all other compositions exhibit velocity strengthening behavior. These data suggest that faults containing these gouge materials at similar conditions will slip aseismically. Different conditions (P, T, P_f , etc) are needed to promote velocity weakening behavior and seismic faulting in these materials.

Carbonate gouge is the strongest while the composite gouge compositions are weakest. Composite gouge weakness is due to strain localization along bands of aligned

pyllosilicates. Flow within the carbonate facilitates rotation of the phyllosilicates and helps to generate compositional layering.

High forcing block porosity can affect sample strength. In saturated experiments, porosity allows pore fluid pressure to escape from the gouge layer, increasing sample strength. In samples with strong or velocity strengthening gouge material and porous forcing blocks, the frictional strength of the gouge material may exceed the fracture strength of the forcing block, causing the forcing block to fail. Thus, the fracture strength of the forcing block, rather than the frictional strength of the gouge material, limits sample strength.

In samples with strong gouge material and a porous forcing block deformation extends into the forcing block, suggesting that natural fault zones in porous country rock may form wider damage zones, or several anastomosing gouge zones (Faulkner et al., 2003).

Works Cited:

Faulkner et al. On the internal structure and mechanics of large strike-slip fault zones: field observations of the Carboneras fault in southeastern Spain. *Tectonophysics* (2003) vol. 367 (3-4) pp. 235-251

Himalayan hinterland-verging superstructure folds related to foreland-directed infrastructure ductile flow: Insights from centrifuge analogue modelling

LAURENT GODIN^a, CHRIS YAKYMCHUK^a, LYAL B. HARRIS^b

^a*Department of Geological Sciences and Geological Engineering, Queen's University, Kingston, Ontario K7L 3N6, Canada*

^b*Institut national de la recherche scientifique, centre - Eau Terre Environnement, 490 de la Couronne, Quebec City, Quebec G1K 9A9, Canada*

Abstract. The orogenic superstructure (SS) and infrastructure (IS) constitute two levels of a mountain belt with contrasting structural styles. In the Nepal Himalaya, N-verging back folds, which oppose the orogenic vergence, dominate the SS. Competing explanations for these folds are tested using scaled centrifuge analogue models employing new materials and computed tomodensitometry (CT scanning) (Fig. 1)^{1,2}. This technique provides insight into the progressive three-dimensional formation of mechanically active, buckle and kink folds of a stratified sedimentary sequence upon migmatitic gneisses in a large hot orogen (Fig. 2). Modelling suggests that SS folding occurs during bulk shortening accompanied by IS thickening before IS flow. Focused erosion then instigates IS lateral flow and stretching, decoupling of the SS, and transposition of the lower SS into a detachment zone. Decoupling at the IS-SS interface separates a SS dominated by older folds and an IS characterised by younger horizontal transposition and stretching of early folds. Extrusive ductile flow of the IS locally modifies fold vergence in the SS. The fold asymmetry is thus controlled by the efficiency of coupling between IS and SS; a low viscosity at the IS-SS interface favours complete decoupling and hinders modification of fold vergence, whereas a higher viscosity IS-SS interface favours fold vergence modification. Modelling supports a tectonic scenario in which Himalayan hinterland-verging folds are the product of early shortening of the SS followed by local modification of fold geometry when the IS subsequently stretches and flows during focused erosion and melt-enhanced IS weakening³.

References

1. Godin, L., Yakymchuk, C. and, Harris, L., *in press*. Himalayan hinterland-verging superstructure folds related to foreland-directed infrastructure plastic flow: insights from centrifuge analogue modelling. *Journal of Structural Geology*, doi:10.1016/j.jsg.2010.09.005
2. Yakymchuk, C., Harris, L., and Godin, L., *in review*. Centrifuge modelling of deformation of a multi-layered sequence over a ductile substrate: 1. Style and 4D geometry of active cover folds during layer-parallel shortening. *Submitted to International Journal of Earth Sciences*.
3. Larson, K. P., Godin, L., and Price, R. A., 2010. Kinematic compatibility in orogens: Linking the Himalayan foreland and hinterland in central Nepal. *Geological Society of America Bulletin*, v. 122, p. 1116-1134, doi:10.1130/B30073.1

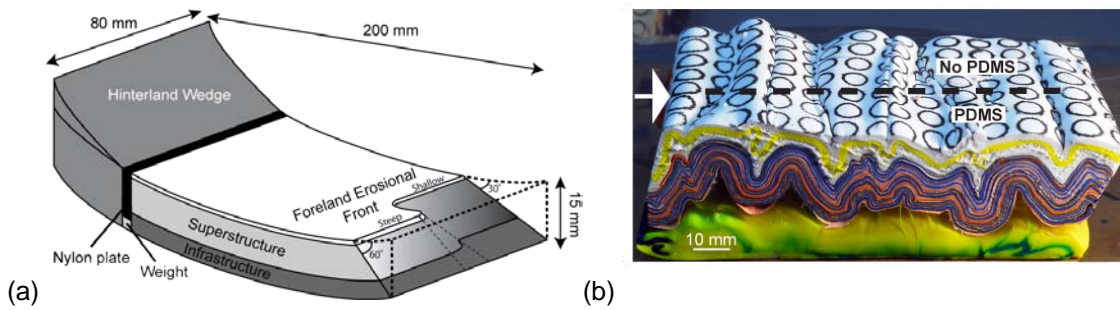


Fig. 1. (a) Model set-up showing the collapsing wedge in the hinterland that activates layer-parallel shortening. Models consist of a 10 mm thick brittle-ductile superstructure overlying a 5 mm thick ductile infrastructure. The portrayed irregular erosion front was created on some models, while others contained an extra layer of polydimethylsiloxane (PDMS), a clear, low density and viscosity polymer, at the infrastructure-superstructure interface that simulates the presence of crustal melts. (b) Example of a model containing one half of PDMS at the interface between the layered sequence and ductile substrate and the other half with no PDMS along this interface.

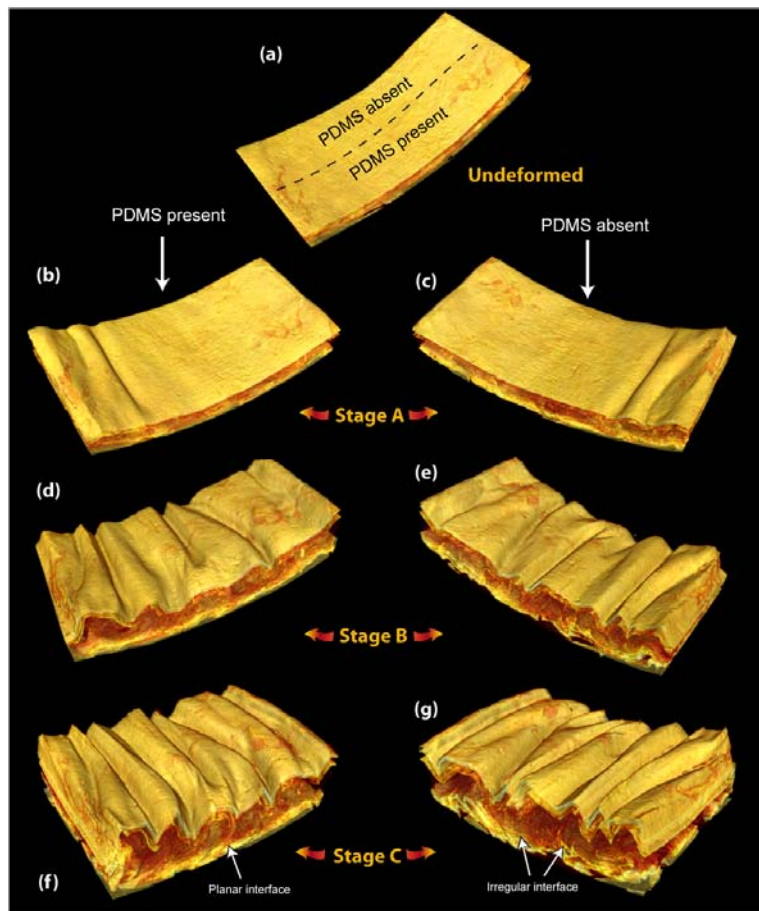


Fig. 2. Example of a sequential CT-images showing each stage of model development: (a) undeformed, (b) and (c) Stage A (19% shortening), (d) and (e) Stage B (31 % shortening), (f) and (g) Stage C (42% shortening). Oblique images show surface deformation features and cross sections along the PDMS-present (b,d,f) and PDMS-absent (c,e,g) halves of the model.

THE HELLROAR CREEK SHEAR ZONE: A MAJOR TECTONIC BOUNDARY IN THE NORTHERN MONASHEE MOUNTAINS OF THE SOUTHEASTERN CANADIAN CORDILLERA

Félix Gervais¹, Andrew Hynes¹, Edward D. Ghent²

¹ *Department of Earth and Planetary Sciences, McGill University, Frank Dawson Adams building, 3450 University Street, Montreal, Quebec, Canada, H3A 2A7*

² *Geoscience, University of Calgary, 2500 University Drive Northwest, Calgary, Alberta, Canada, T2N 1N4*

ABSTRACT

There is a tectonic conundrum in the northern Monashee Mountains. On the one hand, field-based studies indicated that rocks of the area were deformed and metamorphosed as a coherent block, which resulted in three phases of folding and a series of well-defined metamorphic isograds. On the other hand, later geochronological studies pointed to the presence of three domains with distinct timing of metamorphism and deformation, which would imply the presence of unrecognized shear zones or of spatially heterogeneous thermal/fluid flow events.

Our fieldwork conducted east of the town of Blue River (BC; 52°7'N; 118°53'W) revealed the existence of a major SE-striking shear zone, herein named *Hellroar Creek Shear Zone* (HCSZ). We mapped it for ~20 km along the ridge between Mud and Hellroar creeks and then east of Mud Creek valley. The HCSZ is characterized by a large volume (>60%) of highly sheared leucogranite and leucosome, whereas leucogranite in its footwall, although locally as abundant, forms a heterogeneous mesh of highly discordant intrusions. The HCSZ separates a low-strain domain in its footwall, with preserved stratigraphic polarity and dominated by SW- to W-verging structures, from a high-strain domain in its hanging wall, with rocks recording complete transposition by top-to-the-NNE to top-to-the-E shearing. Whereas rocks of its hanging wall are generally at the Sil-Kfs-grade, rocks in its footwall are at the Ky-Ms-grade. Preliminary U-Pb in-situ Mnz geochronology agrees with previous studies and indicates a retrograde path in the Sil field between ~90 and 75 Ma in hanging wall rocks, while footwall rocks were on a prograde path in the Ky field. The presence of pods of footwall rocks, with diameters ranging from < 2 m to >50 m, included in highly sheared rocks of the HCSZ, highlights the complexity of the zone.

Interestingly, the HCSZ is located along-strike from, and separates the same lithologic packages as the boundary between two of the geochronological domains previously identified ~20 km to the SE. We thus propose that the HCSZ connects with this boundary to form a >40 km long shear zone. The HCSZ is interpreted as the base of a channel flow system that was active for >30 Myr in the Late Cretaceous. If this interpretation is correct, the HCSZ would be the NE extension of the Monashee décollement that bounds the western flank of the Monashee Complex, ~60 km to the SSW.

Mechanisms of Strain Localization within the 2004-2008 Mt. St. Helens lava domes: The role of effusion rate?

B.A. Friedlander, L.A. Kennedy, J.K. Russell, J. Pallister

Degassed, high viscosity magmas commonly erupt from volcanic vents to produce mounds, domes and spines of partly to fully crystallized lava. Although lava domes are generally products effusive styles of eruption, these systems have the capacity to rapidly switch from effusive to explosive behavior. Soufriere Hills, Montserrat and Unzen, Japan volcanoes have each demonstrated the ability to oscillate between effusive growth of lava domes and the gravitational collapse of these unstable landforms, leading to explosive pyroclastic eruptions.

Mount St. Helens reawakened 24 years after erupting in the 1980's to produce a series of 7 dacitic lava domes and spines from 2004-2008. The rate of extrusion of lava domes peaked at $6 \text{ m}^3/\text{day}$ in November 2004 and subsequently slowed to $< 0.6 \text{ m}^3/\text{day}$ in February 2006. These early spines were mantled by 1-3 meters of fault gouge and were accompanied by a consistent "drum beat" microseismicity that was monitored closely by the USGS Cascades Volcano Observatory.

Here we present field, petrographic and microstructural observations on the nature of deformation attending the extrusion of the 2004-2006 dacite lava domes at Mount St. Helens. Specifically, we have produced a series of metre-scale maps showing the transition in structural state from the massive, undeformed dacite to the cataclasite and gouge zones of Spine 4, 5 and 6. These maps elucidate the strain partitioning and zones of deformation. Samples collected from across these zones are currently being studied to recover the microstructural deformation mechanisms attending the extrusion of these dacite spines.

Between spines, the shear zones vary in thickness and range in thickness from one to three meters. The outermost damage zones range in thickness from 1-100cm of fault gouge composed of fractured dacite and wall rocks interleaved with layers of fine to coarse-grained slickensides. Below the gouge, spines 4 and 5 show mostly brittle deformation with the core of the shear zone composed of Reidel fractures that evolve with higher strain into Y-foliated fabrics. At Spine 6, strain is also manifested by the formation of a brittle gouge and by the formation of a ductile mylonitic- texture suggesting a brittle-ductile transition within the margins of the extruded lava dome. Below these 1-3 meter thick fault zones, the interior of each spine is comprised of flow banded to massive dacite lava.

Lastly, we compare our field observations of the strain associated with extrusion of the lava domes to the observed rates of extrusion. This comparison will elucidate the effect of extrusion rate of magma (e.g., strain rate) on deformation mechanisms within the cylindrical shear zones. Ultimately, our intent is to correlate effusion rates, drumbeat seismicity and deformation styles to address what mechanisms are the causes of the seismicity and what other aseismic mechanisms accompany and attend the Mount St. Helens lava dome extrusion.

TITLE: MULTISCALE STRUCTURAL ANALYSIS OF THE SUNYANI BASIN, GHANA

NAME: Prince Ofori Amponsah
Department of Earth Sciences, University of Ghana

Current Address: Department of Earth Sciences, Simon Fraser University, 8888 University Drive, Burnaby, BC, V5A 1S6

Email: pamponsa@sfu.ca

ABSTRACT:

The Paleoproterozoic Sunyani basin of the Birimian terrane in Ghana is currently a prospective terrane for gold Exploration. For efficient gold exploration, understanding the regional tectonic evolution of the area is critical. The Basin is lithologically composed of metasedimentary rocks, granitic intrusions and minor volcanic basaltic rocks. Deciphering the structural evolution of the terrane has been made possible by a multiscale approach. A compilation of results from the structural analysis undertaken during geological field mapping and analysis of geophysical aeromagnetic and radiometric data shows that the study area has experienced two deformation events, referred to as D_1 and D_2 . The D_1 deformation is characterized by an initial S_1 foliation which is parallel to the axial planes of most of the microfolds, which also contain a stretching lineation. D_2 marks the major deformation in the study area. It is characterized by regional sinistral strike-slip faults, which included shearing that produced regional S-structures and S-C fabrics shown by the rocks found in the shear zones and associated minor folding events. The S-C structures give an indication of progressive deformation produced by sinistral strike-slip simple shear.